Electronic Supplementary Material (ESI) for Environmental Science: Advances.


# Supporting Information

## Tracing the origin of elevated springtime atmospheric sulfate on the Southern Himalayan-Tibetan Plateau

*Sanjeev Dasari[1#*], Guillaume Paris[2], Qiaomin Pei[3], Zhiyuan Cong[3], David Widory[4*]*

[1]Institut des Géosciences de L'Environnement (IGE), University Grenoble Alpes, CNRS, IRD, Grenoble INP, Grenoble 38000, France

[2]Université de Lorraine, CNRS, CRPG, Nancy 54000, France

[3]Key Laboratory of Tibetan Environment Changes and Land Surface Processes, Institute of Tibetan Plateau Research, Chinese Academy of Sciences, Beijing 100101, China

[4]GEOTOP/ Université du Québec à Montréal, Montréal H3C 3P8, Canada

[#]*Now at* Department of Earth Sciences, University of Oxford, Oxford OX1 3AN, United Kingdom

**Corresponding authors:* sanjeev.dasari@earth.ox.ac.uk, widory.david@uqam.ca

**Supporting information includes**: 14 Pages, 1 Notes, 7 Figures, 1 Table

# Contents

## *Supplementary Notes*

### Note S1. Chemical and S multi-Isotope measurements for $PM_{2.5}$ aerosol samples collected at QOMS

**Water-soluble ion analysis:** A filter punch was soaked in 10 mL of Milli-Q water added by ultrasonification for 30 min. The water extracts were filtered using a 0.45μm Millipore filters. An ion chromatograph instrument operating at 1.0 ml $min^{-1}$ was used for this purpose [Metrohm IC]. Calibration of the instrument was done using commercial standards (~10 to 100 parts per million). Standard stock solutions from analytical grade reagents and salts were used for quality assurance of the analytical data (within 5%). Blank filters were also analysed with the samples and the concentrations in the aerosol samples were suitably corrected for contribution from the blanks.

**Metal analysis:** A filter punch was digested with ultra-pure mixing of nitric acid, hydrogen peroxide, and hydrofluoric acid (6 mL $HNO_3$ + 2 mL $H_2O_2$ + 1 mL HF) at 180°C for 6 hours adapted from the protocol detailed elsewhere[1]. After filtration through a 0.45 μm pore filter, metal concentrations were measured by inductively coupled plasma-mass spectrometry (Agilent 8900 Triple Quadrupole ICP-MS). Quality control was performed by repeated analysis of multi-element calibration standards (SCP science) along with blank correction to report the aerosol concentration.

**S multi-isotope analysis:** Column chemistry is used to extract sulfate from the filters as discussed in our previous publication[2]. After purification, the extracts were analyzed for S multi-isotopes at CRPG on a Neptune Plus MC-ICP-MS (Thermo Fisher Scientific Neptune Plus) coupled with a desolvation membrane (Aridus II, Cetac) to reduce the interference of oxides and hydrides on the masses $^{32}S$, $^{33}S$ and $^{34}S$ and to increase the sensitivity to the signal[3,4]. The Paris et al., protocol[3] is used for analysis by standard-sample bracketing using an in-house $Na_2SO_4$ standard to correct for instrumental isotope fractionation. Each sample was run a minimum of four independent times, usually five, with each run consisting of fifty acquisition of 4.2 seconds. The sample requirement for this method is ~40 nmol and as such this could become a preferable method for high-resolution S multi-isotope analysis.

The reported values (see Supplementary Table S1) are given as $1\sigma$ (standard deviation) of at least 5 independent measurements on the Neptune for a given sample. Assessment of quality control, accuracy, and precision of this method for S multi-isotope analysis in aerosols has been discussed in detail in our recent publication[2]. The triple sulfur isotopes ($^{32}S$, $^{33}S$, $^{34}S$) are reported relative to the Vienna-Canyon Diablo Troilite (V-CDT) standard. Quality control using various standards and three separate seawater samples was conducted as detailed elsewhere[2], Procedural blanks were also run with each set of samples and represent less than 1% of the total sulfur of a sample.

## *Supplementary Figures*

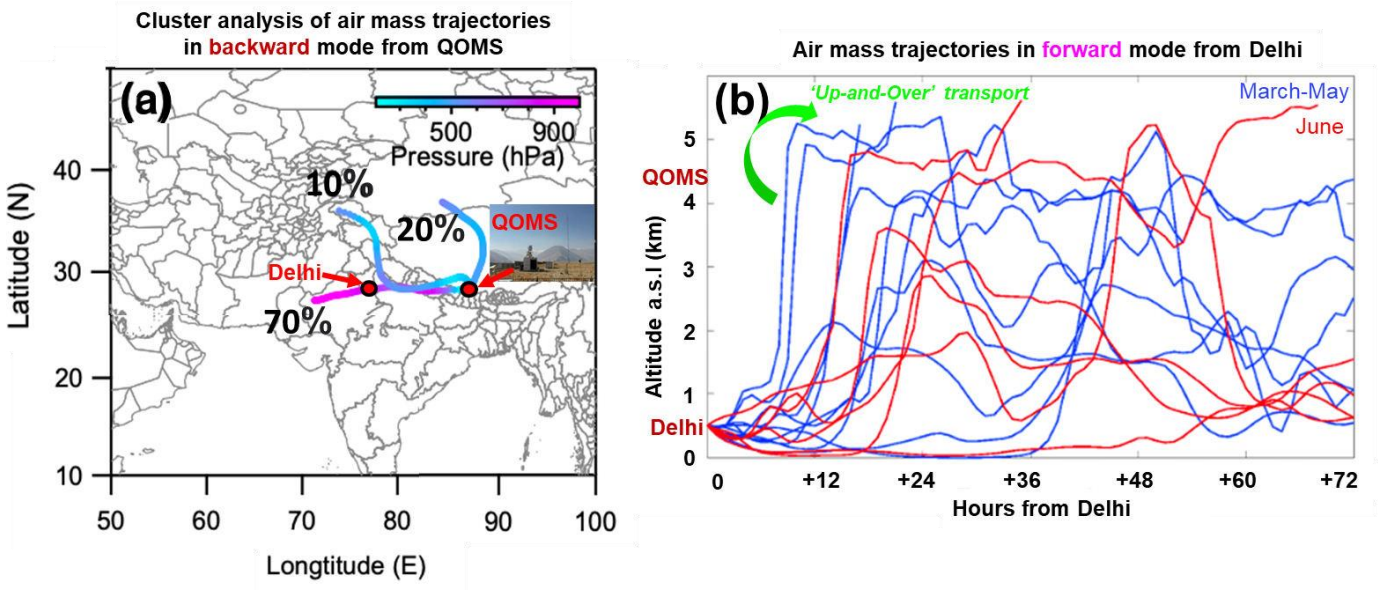


**Figure S1. Air mass transport at QOMS during spring of 2021.** (a) Cluster analysis of 7-day air mass back-trajectories computed hourly using NOAA Hybrid Single-Particle Lagrangian Integrated Trajectory model (HYSPLIT) version 4[14,15]. Over the course of the campaign the air masses were predominantly from the S Asian region. As such, synoptic sampling was possible as air masses were linking the sites Delhi and QOMS, (b) Forward trajectories were computed from Delhi for which the height of air masses is shown (for 72 h). the distinct springtime feature 'up-and-over' transport can be seen wherein air masses are rapidly transported to higher altitudes from the Indo-Gangetic Plain to the HTP.

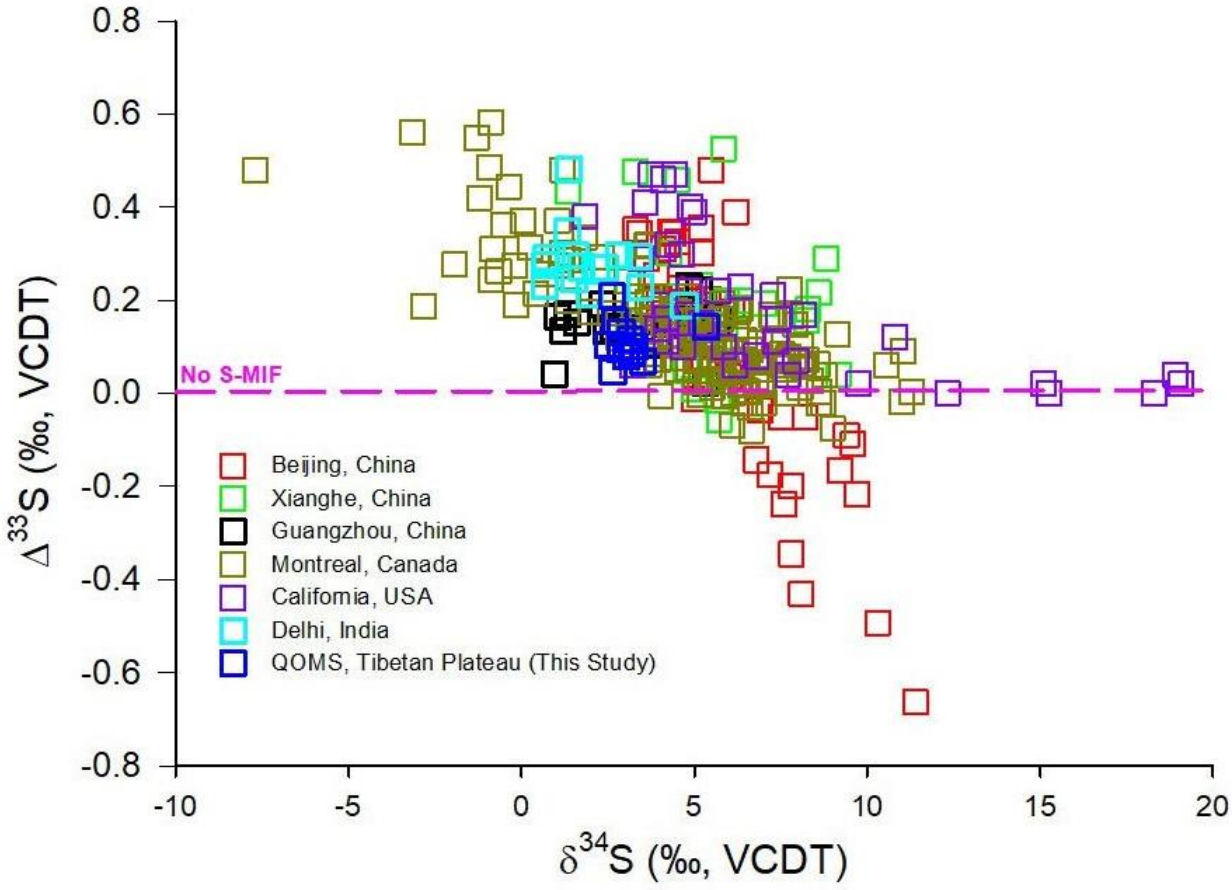


**Figure S2. A comparison of aerosol sulfur isotope anomalies from published records**[2,6-11].

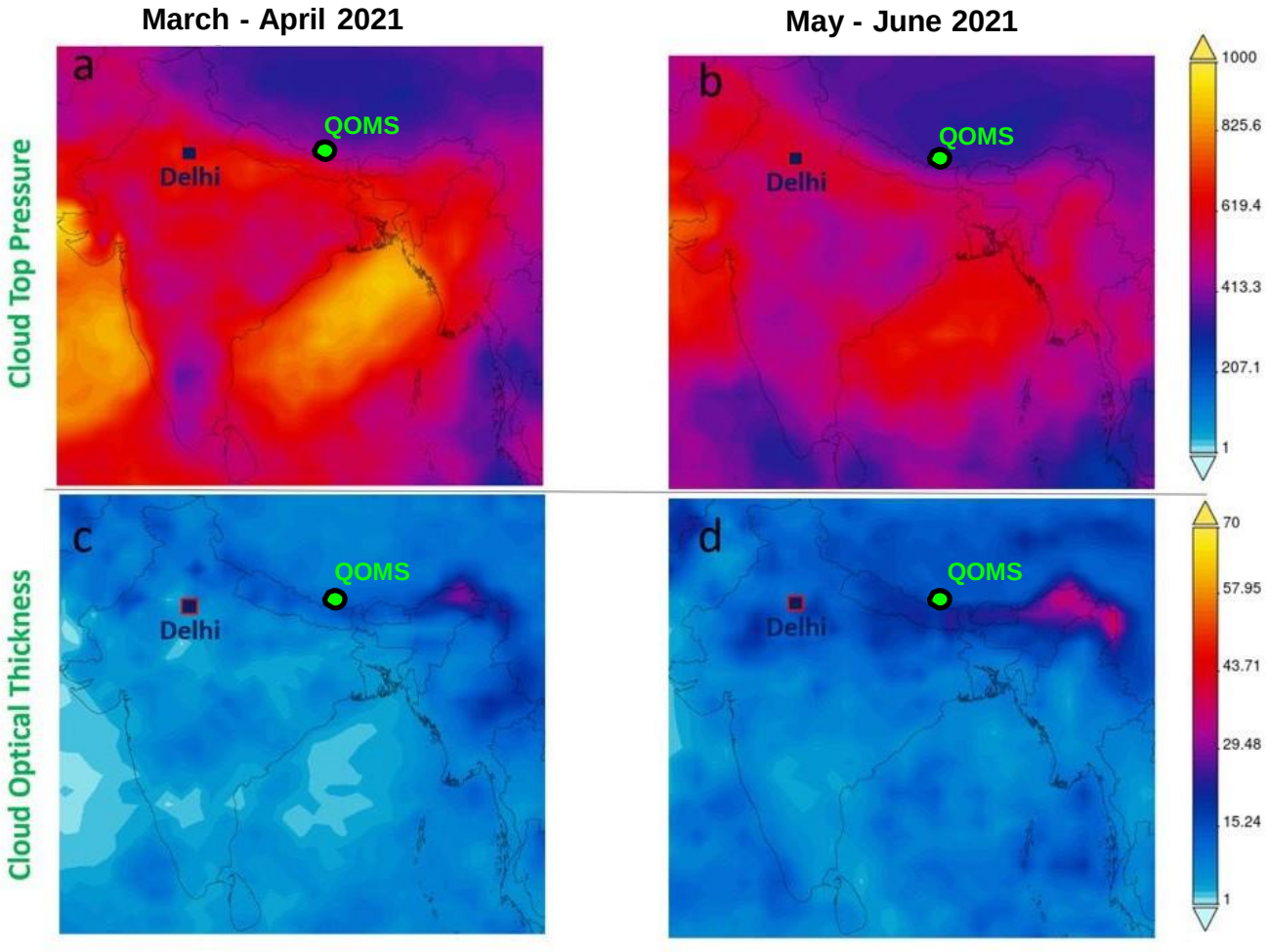


**Figure S3. Time-averaged map of cloud parameters**. MODIS AQUA, TERRA-based [product MYD08_D3 v6.1, MOD08_D3 v6.1][16] monthly mean of (a, b) cloud top pressure [in mb] and (c,d) cloud optical properties shown for the months of March-April and May-June 2021 over the S Asian region [https://giovanni.gsfc.nasa.gov/giovanni/].

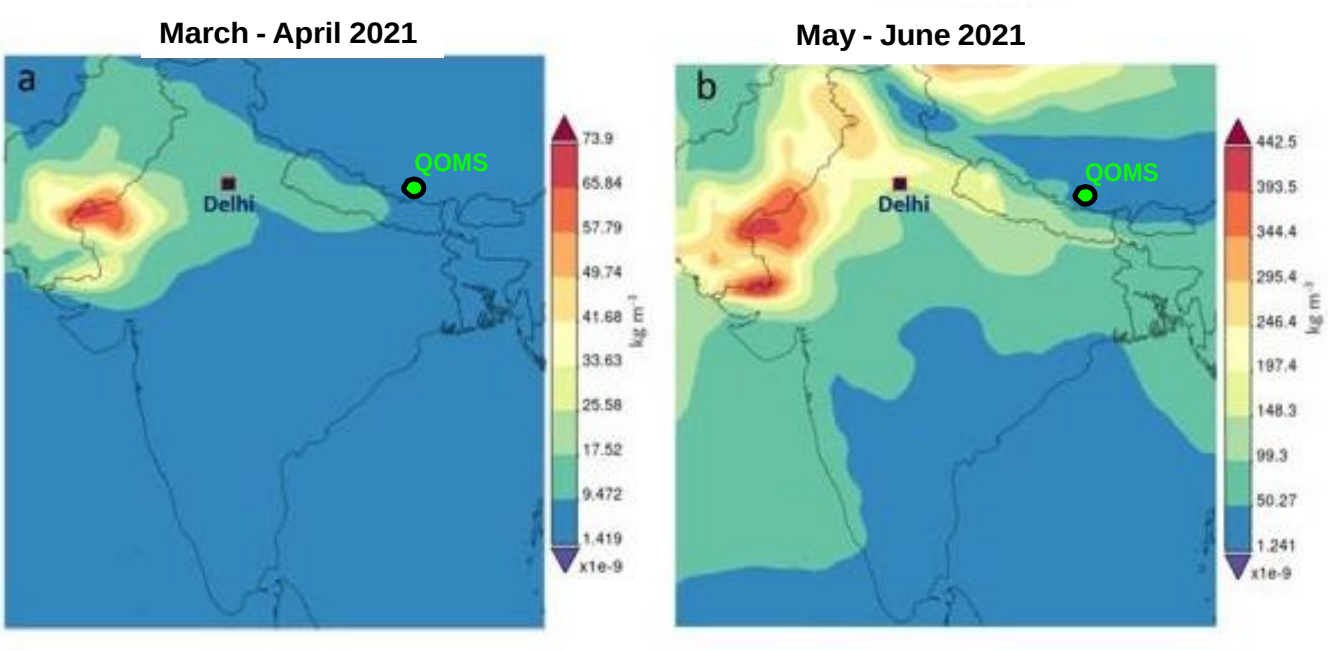


**Figure S4. Time-averaged map of dust surface mass concentration.** Computed monthly 0.5°x0.625° grid using the MERRA-2 model M2T1NXAER v5. 12.4 [https://giovanni.gsfc.nasa.gov/giovanni/][17].

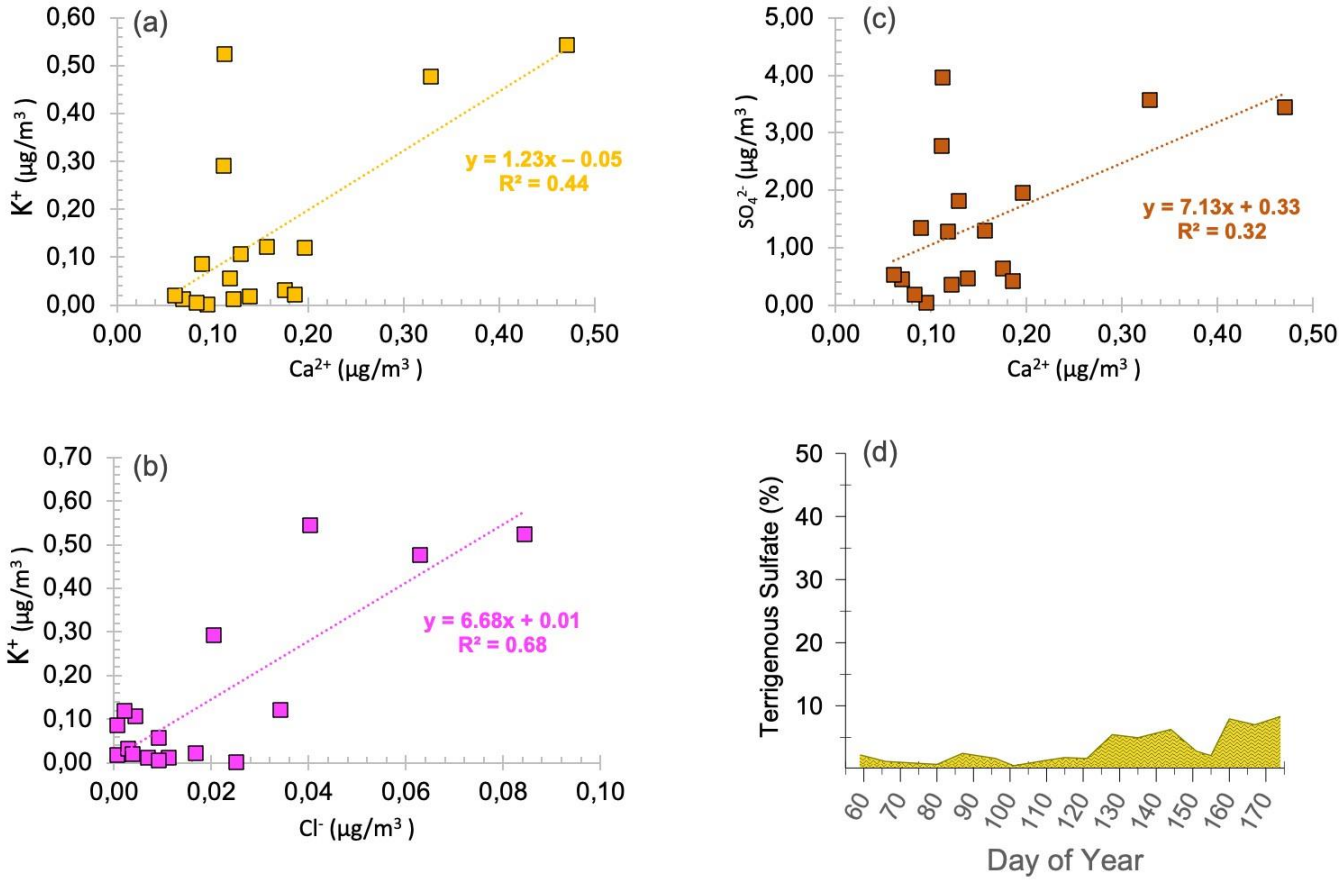


**Figure S5. Establishing the role of mineral dust and biomass burning through correlations of water-soluble ions at QOMS during spring of 2021.** The fraction of terrigenous sulfate in total sulfate is shown for the QOMS site. This fraction is calculated based on the ratio of $SO_4^{2-}$-to-$Ca^{2+}$ concentrations in regional soil to the same in sampled aerosol[5].

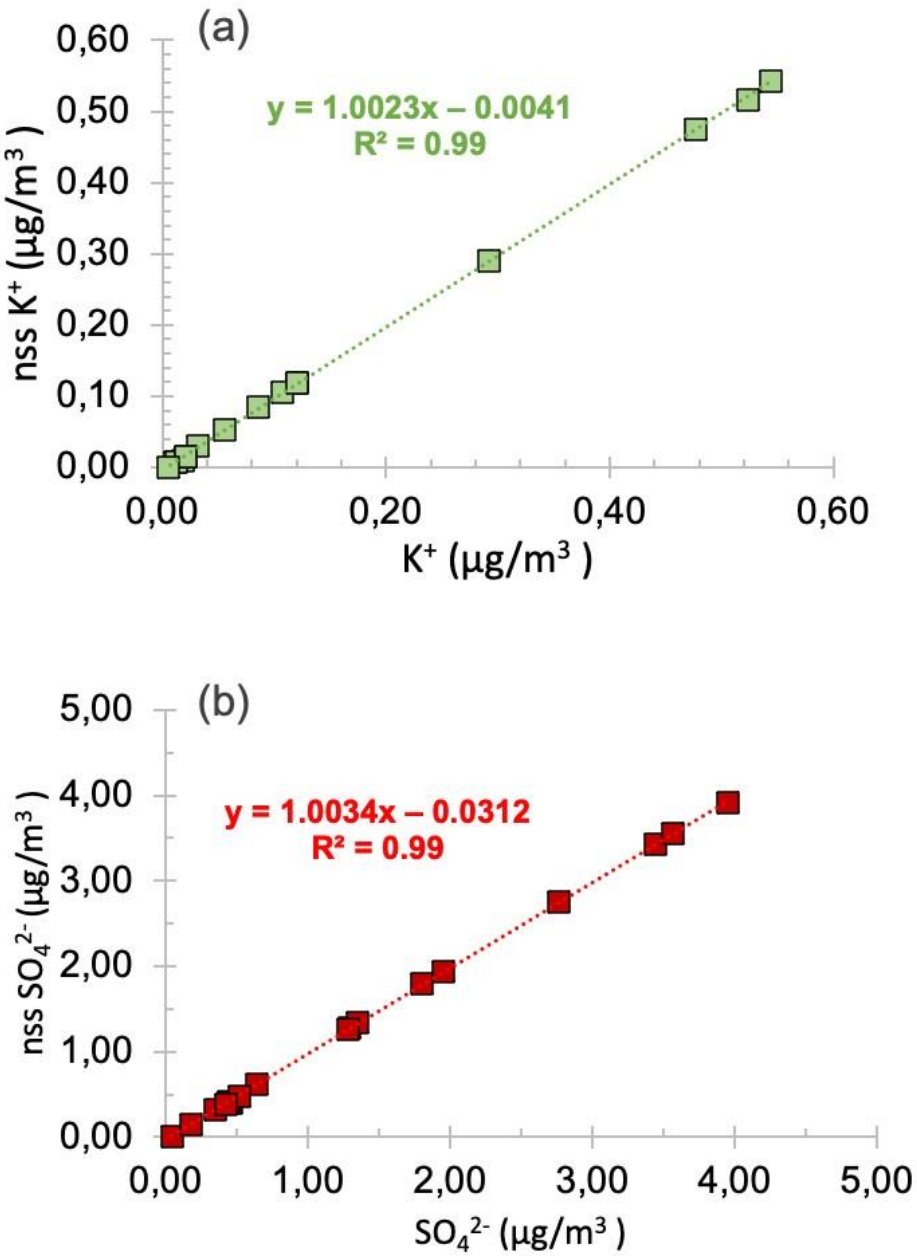


**Figure S6. Marine influence on sulfate and potassium concentrations at QOMS.** The non-sea salt potassium and sulfate concentrations are shown along with the total potassium and sulfate concentrations.

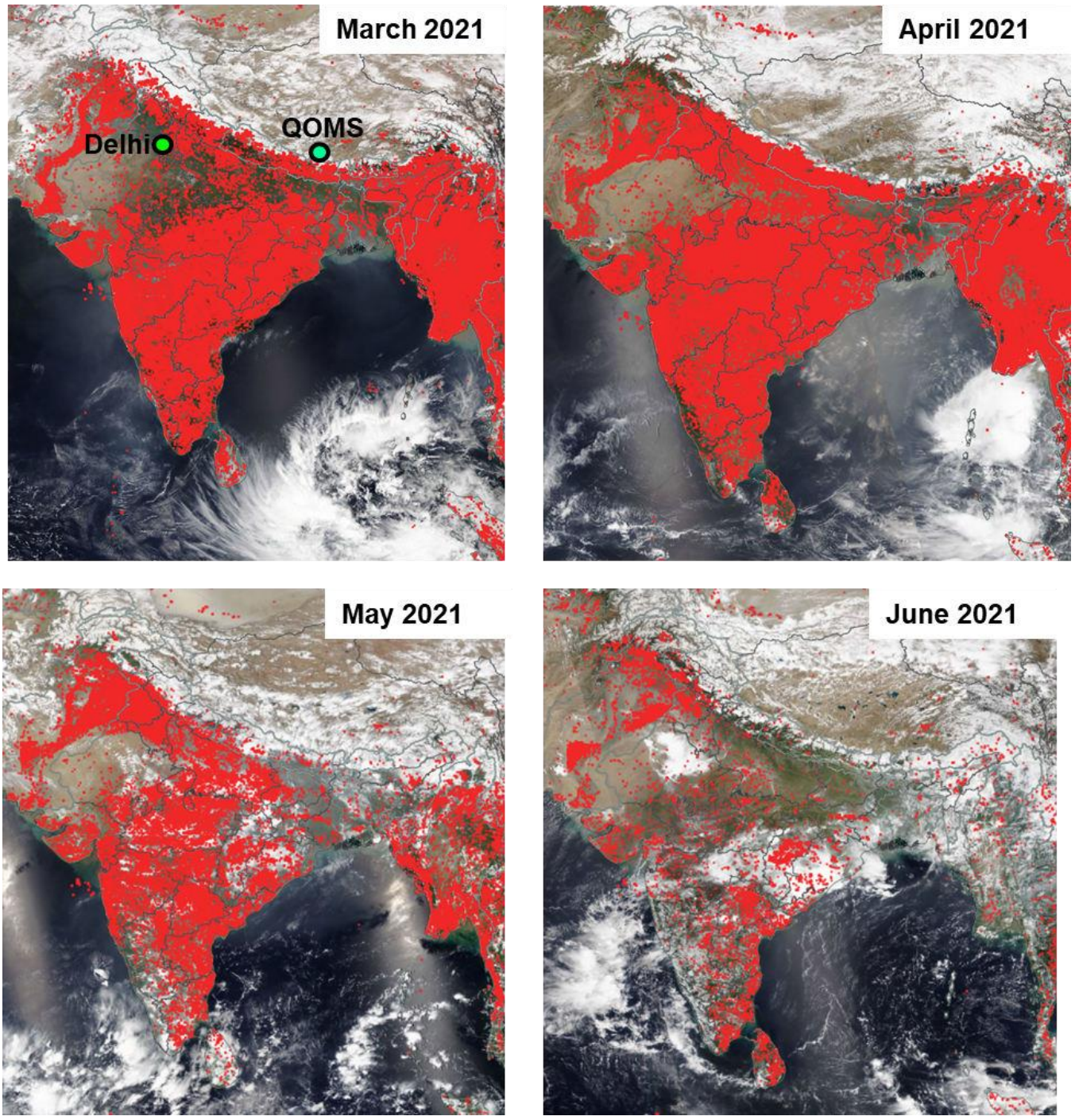


**Figure S7. Open burning in S Asia during spring of 2021.** The data is obtained from the Fire Information for Resource Management System (FIRMS)[18] service of NASA https://firms.modaps.eosdis.nasa.gov/.

**Table S1. Sampling details along with concentrations of water-soluble ions and S multi-isotope composition for samples collected with a frequency of 4-days at QOMS during spring 2021.** Note that due to a lack of availability of sample material for isotopic analysis, the samples prior to April could not be measured for the same. However, based on a recent study[12], it is argued that the period from April till June is rather found to be devoid of influence from stratospheric intrusions (please refer to Figure 4 in Wang et al., 2021) and is precisely when a maximum influx of biomass burning aerosols is found at QOMS[13]. As such is the most suited scientifically to study the influence of biomass burning on the observed S-MIF signals at QOMS.

| Sampling start date | $Na^+$ [µg/m$^3$] | $K^+$ [µg/m$^3$] | $Ca^{2+}$ [µg/m$^3$] | $SO_4^{2-}$ [µg/m$^3$] | $\delta^{34}$ [‰] | s.d. | $\Delta^{33}$ [‰] | s.d. |
|---|---|---|---|---|---|---|---|---|
| 28/02/2021 | 0.07 | 0.12 | 0.16 | 1.29 | NA | NA | NA | NA |
| 07/03/2021 | 0.05 | 0.09 | 0.09 | 1.35 | NA | NA | NA | NA |
| 21/03/2021 | 0.06 | 0.29 | 0.11 | 2.77 | NA | NA | NA | NA |
| 28/03/2021 | 0.04 | 0.54 | 0.47 | 3.44 | NA | NA | NA | NA |
| 06/04/2021 | 0.07 | 0.48 | 0.33 | 3.57 | 2.62 | 0.09 | 0.21 | 0.03 |
| 11/04/2021 | 0.19 | 0.52 | 0.11 | 3.96 | 2.71 | 0.05 | 0.15 | 0.03 |
| 19/04/2021 | 0.06 | 0.11 | 0.13 | 1.81 | 3.27 | 0.05 | 0.10 | 0.03 |
| 25/04/2021 | 0.06 | 0.12 | 0.20 | 1.96 | 2.87 | 0.03 | 0.10 | 0.02 |
| 01/05/2021 | 0.09 | 0.06 | 0.12 | 1.29 | 2.64 | 0.04 | 0.05 | 0.04 |
| 08/05/2021 | 0.24 | 0.02 | 0.14 | 0.46 | 2.50 | 0.05 | 0.10 | 0.04 |
| 15/05/2021 | 0.05 | 0.03 | 0.18 | 0.64 | 2.89 | 0.04 | 0.13 | 0.02 |
| 24/05/2021 | 0.11 | 0.01 | 0.12 | 0.35 | 3.13 | 0.04 | 0.11 | 0.04 |
| 31/05/2021 | 0.12 | 0.01 | 0.07 | 0.45 | 3.20 | 0.01 | 0.09 | 0.02 |
| 04/06/2021 | 0.15 | 0.02 | 0.06 | 0.52 | 3.04 | 0.06 | 0.08 | 0.05 |
| 09/06/2021 | 0.15 | 0.02 | 0.19 | 0.42 | 3.53 | 0.03 | 0.07 | 0.03 |

| | | | | | | | | |
|---|---|---|---|---|---|---|---|---|
| 16/06/2021 | 0.14 | 0.00 | 0.09 | 0.05 | 5.34 | 0.04 | 0.14 | 0.02 |
| 23/06/2021 | 0.13 | 0.00 | 0.08 | 0.18 | 3.20 | 0.07 | 0.09 | 0.02 |

## *References*


1. X. Wu, B. Chen, T. Wen, A. Habib and G. Shi, *J. Environ. Sci.* 2020, **87**, 1-9.

2. S. Dasari, G. Paris, B. Saar, Q. Pei, Z. Cong and D. Widory, *Environ. Sci. & Technol. Lett.* 2022, **9**, 604-610.

3. G. Paris, A. L. Sessions, A. V. Subhas and J. F. Adkins, *Chem. Geol.* 2013, **345**, 50–61.

4. G. Paris, W. W. Fischer, J. E. Johnson, S. M. Webb, T. M. Present, A. L. Sessions and J. F. Adkins, *Geochem. Cosmo. Acta.*, 2020, **285**, 1-20.

5. X. Han, Q. Guo, C. Liu, P. Fu, H. Strauss, J. Yang, J. Hu, L. Wei, H. Ren, M. Peters and R. Wei, *Sci. Rep.* 2016, **6**, 29958.

6. X. Han, Q. Guo, H. Strauss, C. Liu, J. Hu, Z. Guo, R. Wei, M. Peters, L. Tian and J. Kong, *Envi. Sci. Tech.* 2017, **51**, 7794–7803.

7. Z. Guo, Z. Li, J. Farquhar, A. J. Kaufman, N. Wu, C. Li, R. R. Dickerson and P. Wang, *J. Geophys. Res.* 2010, **115**, D00K07.

8. D. Au Yang, P. Cartigny, K. Desboeufs and D. Widory, *Atmos. Chem. Phys.* 2019, **19**, 3779-3796.

9. M. Lin, X. Zhang, M. Li, Y. Xu, Z. Zhang, J. Tao, B. Su, L. Liu, Y. Shen and M. H. Thiemens, *Proc. Natl. Acad. Sci.* 2018, **115**, 8541-8546.

10. A. B. Romero and M. H. Thiemens, *J. Geophys. Res.* 2003, **108**, 4524.

11. B. Yin, X. Yu, X. Lin, Z. Zhang, Y. Zhang and M. Lin, *ACS Earth Space Chem.*, 2023, **7**, 800-811.

12. K. Wang, S. Hattori, M. Lin, S. Ishino, B. Alexander, K. Kamezaki, N. Yoshida and S. Kang, *Atmos. Chem. Phys.*, 2021, **21**, 8357-8376.

13. Z. Cong, K. Kawamura, S. Kang, and P. Fu, *Sci. Rep.*, 2015b, **5**, 1-7.

14. A. F. Stein, R. R. Draxler, G. D. Rolph, B. J. B. Stunder, M. D. Cohen and F. Ngan, *Soc., 2015, **96**, 2059-2077.*

15. G. Rolph, A. Stein and B. Stunder, *Envi. Model. Soft., 2017, **95**, 210-228,*

16. S. Platnick, P. Hubanks, K. Meyer, and M. D. King, MODIS Atmosphere L3 Monthly Product (08_L3). NASA MODIS Adaptive Processing System, Goddard Space Flight Center http://dx.doi.org/10.5067/MODIS/MOD08_M3.006 (Terra) http://dx.doi.org/10.5067/MODIS/MYD08_M3.006 (Aqua) Accessed: **[*20 May 2023*]**.

17. Goddard Earth Sciences Data and Information Services Center (GES DISC).MERRA-2 tavgM_2d_aer_Nx: 2d,Monthly mean,Time-averaged,Single-Level,Assimilation,Aerosol Diagnostics V5.12.4, Greenbelt, MD, USA, Goddard Earth Sciences Data and Information Services Center (GES DISC),https://disc.gsfc.nasa.gov/datasets/M2TMNXAER_5.12.4/summaryDOI: 10.5067/FH9A0MLJPC7N Accessed: **[*20 May 2023*]**.

18. MODIS Collection 6 Hotspot / Active Fire Detections MCD14ML distributed from NASA FIRMS. Available on-line https://earthdata.nasa.gov/firms Accessed: **[*20 May 2023*]**.